https://doi.org/10.5194/essd-2020-397
Preprint. Discussion started: 19 February 2021

Open Access Earth System Science Data Discussions

ERA5-based database of Atmospheric Rivers over Himalayas

Munir Ahmad Nayak*, M. Farooq Azam, Rosa Vellosa Lyngwa

[1]Discipline of Civil Engineering, Indian Institute of Technology Indore, Simrol, Indore, Madhya Pradesh, India-453552

Correspondence to: Munir Ahmad Nayak, munir_nayak@iiti.ac.in

https://doi.org/10.5194/essd-2020-397
Preprint. Discussion started: 19 February 2021

Open Access Earth System Science Data Discussions

1 Abstract

Atmospheric Rivers (ARs) —long and narrow transient corridors of large horizontal moisture flux in the lower troposphere— are known to shape the hydrology of many regions around the globe. Heavy precipitation and flooding are often observed over many mountainous regions when the moisture-rich filaments impinge upon the elevated topographies. Although ARs and their impacts over many mountainous regions are well documented, their existence over the Himalayas and importance to the Himalayan hydrology have received negligible attention in the scientific literature. The Himalayas support more than a billion population in the Indian subcontinent, sustain the region's biodiversity, and play important roles in regulating the global climate.

In this study, we develop a comprehensive database of ARs over the Himalayas using the European Reanalysis fifth generation (ERA5) fields of humidity and winds. The AR database consists of the dates and times of ARs from 1982 to 2018, their duration, major axes, and intensities and categories. We find that majority of intense ARs are associated with extreme precipitation widespread over the Ganga and Indus basins of the Himalayas, suggesting that ARs have profound impacts on the hydrology of the region. The AR database developed here is envisioned to help in exploring the impacts of ARs on the hydrology and ecology of the Himalayas. For this, we provide a few brief future perspectives on AR-Himalayas relationships.

The data developed in this study has been uploaded to the Zenodo repository at https://doi.org/10.5281/zenodo.4451901 (Nayak et al., 2021). The data are also included in the Supplemental Information for easier access.

https://doi.org/10.5194/essd-2020-397
Preprint. Discussion started: 19 February 2021

Open Access Earth System Science Data Discussions

2 Introduction

2.1 Brief overview of Atmospheric River studies over mountainous regions

Owing to the uneven solar heating of the earth's surface, net transports of atmospheric energy and moisture result from the tropics to the polar regions. Newell et al., (1992) observed driver-like filaments in the maps of specific humidity and horizontal water vapor flux in the lower troposphere, which they named as "tropospheric rivers". The features were later termed as "Atmospheric Rivers" (ARs) by Zhu & Newell, (1998), who estimated that more than 90% of the poleward flux of water vapor in the extratropical atmosphere at any time instant happens through only a few transient (less than ten) ARs that occupy ~10% of the global circumference at a given latitude. Two decades later, after significant research breakthroughs in AR science, a more formal and thorough definition was introduced in the Glossary of Meteorology (Ralph et al., 2018). The most definitive feature of ARs is the strong horizontal water vapor transport in long and relatively narrow bands in the lower atmospheric levels (< 3km from the surface of Earth). ARs are typically associated with extratropical cyclones, many ARs, however, transport moisture from the tropical latitudes and are associated with tropical cyclones (Cordeira et al., 2013; Ralph et al., 2011; Sodemann and Stohl, 2013; Stohl et al., 2008).

In the last two decades, ARs have gained increased scientific attention due to their societal impacts in the form of intense storms and flooding events associated with them. Over many regions around the globe, ARs are known to be among the key drivers of major flooding events and other extreme precipitation related disasters (west coast of USA (Dettinger et al., 2011; Dettinger and Cayan, 2014; Young et al., 2017); Europe (Lavers et al., 2012; Lavers and Villarini, 2013b, 2015a); Japan (Kamae et al., 2017)). At the same time, moisture transported in ARs has been shown to be a major source of beneficial water to sustain municipal water systems, agricultural systems, and the ecosystem (Florsheim and Dettinger, 2015; Guan et al., 2010), and at times, they supply essential water to recover from droughts (Dettinger et al., 2011). In US West Coast mountainous regions, a major fraction (more

https://doi.org/10.5194/essd-2020-397
Preprint. Discussion started: 19 February 2021


Open Access Earth System Science Data Discussions

than 30%) of winter snowpack is shown to be accumulated by only a few AR storms (Guan et al., 2010; Guan and Chan, 2006).

In mountainous ranges, the impacts of ARs are pronounced when the moisture-laden air is lifted vertically by the elevated topography, such is the case with the US West Coast, parts of Europe, and many other regions. In the Indian subcontinent, an important barrier to atmospheric flow is the Himalayan mountain range; however, the role of ARs in the hydrology of the region is essentially unexplored.

2.2 Himalayan water resources under climate change

The Himalayan mountain range is home to the world's highest glaciers therefore rightly called the water tower of Asia or 'Third Pole' (Bolch et al., 2019). The Himalayan river basins of Indus, Ganga, and Brahmaputra are among the most melt-water dependent rivers systems on Earth and satisfy the water requirements of more than a billion people (Immerzeel et al., 2020; Pritchard, 2019). There are ~40,000 glaciers covering ~41,000 km^2 area in the Himalayas with an estimated ice volume of 3500 km^3 (Bolch et al., 2019; Farinotti et al., 2019). The frozen water storage in these glaciers and seasonal snow covers directly affect the runoff in the Himalayan river basins hence is important to the downstream population for irrigation, hydropower, sanitation, and industries (Biemans et al., 2019; Bolch et al., 2019; Momblanch et al., 2019).

Under the ongoing global warming, water towers of the world's mountain ranges are under threat including the Himalayas —Indus Basin being the most vulnerable (Huss and Hock, 2018; Immerzeel et al., 2020). Glacio-hydro-meteorological investigations in the Himalayas are scarce compared to other mountainous regions on Earth because of inherent challenges in maintaining the monitoring networks due to rough climatic conditions and challenging access to the glaciers (Azam et al., 2018). A few studies, generally using low altitude meteorological data, revealed increasing temperature trends over the past 5–6 decades with varying rates in different regions whereas

https://doi.org/10.5194/essd-2020-397
Preprint. Discussion started: 19 February 2021


Open Access Earth System Science Data Discussions

precipitation did not show any particular spatiotemporal trend in the Himalayan region (Krishnan et al., 2019).

In response to the global as well as regional warmings (Banerjee and Azam, 2016; Krishnan et al., 2019; Pörtner et al., 2019), glaciers have been found to be diminishing in the Himalayas over the past 5–6 decades (Azam et al., 2018; Bolch et al., 2019). However, the shrinkage rates are heterogeneous: negative mass balances in the eastern, central, and western Himalaya and near-balance state in the Karakoram range (Azam et al., 2018; Bolch et al., 2019; Brun et al., 2017). These changes caused considerable alteration to the volumes and seasonality in river runoff, affecting the agriculture, hydropower production, and even sea level (Biemans et al., 2019; Farinotti et al., 2019; Momblanch et al., 2019). For instance, river flow reduction by 1% is expected to bring roughly 3% reduction in hydropower production (Laghari, 2013). Glacier changes are also linked with potential hazards such as glacial lake outburst floods (Bhambri et al., 2020; Veh et al., 2019). Besides, the Himalayan rivers are trans-boundary in nature and any future change in runoff regimes may give rise to demands for reworking water-sharing treaties among surrounding countries (Molden et al., 2017)

2.3 Lack of studies on ARs in Himalayas

Over the years, especially since the availability of satellite-based imagery, ARs have garnered numerous important works that have significantly advanced the scientific understanding of the hydro-climatology of many mountainous regions on Earth. For example, after understanding and recognizing the presence and impacts of ARs, it has now been possible to more clearly define and narrow the challenges in water management of the western US (Ralph et al., 2019; Steinschneider et al., 2015; Steinschneider and Brown, 2012). Many previously unexplored mountainous regions begin to appreciate the role of ARs in shaping the regional hydrology (Chen et al., 2019; Wille et al., 2019).

Knowledge of AR presence over the Himalayan mountain range and their hydrological impacts is sparse. In some parts of the India continent, however, a few studies on ARs have emerged recently. Lakshmi & Satyanarayana, (2019) observed that the heavy precipitation events that led to major

https://doi.org/10.5194/essd-2020-397
Preprint. Discussion started: 19 February 2021


Open Access Earth System Science Data Discussions

105 flooding in November and December of 2015 over Chennai city in south-east India were associated
106 with ARs. Thapa et al., (2018) studied the association of extreme precipitation over the western Nepal
107 with ARs penetrating the transect at 80.25°E from 27°N to 30.75°N, which intersects the Himalayan
108 arc used in this study only at one location. They highlighted that a significant fraction (more than 35%)
109 of annual maximum and seasonal maximum precipitation events happened during the presence of
110 ARs. Liang & Yong, (2020) used horizontal integrated water vapor transport (IVT) threshold of
111 $500\ kgm^{-1}s^{-1}$ to identify ARs and discussed their impacts over the Asian Monsoon regions, which
112 also covers the Indian subcontinent. However, the Himalayas, especially, the western Himalaya, are
113 less affected by the main strong monsoon flows, and IVT of $500 kgm^{-1}s^{-1}$or higher rarely happens
114 over the region (as shown in Figure 2 of Liang & Yong, (2020)). Consequently, the study did not
115 identify ARs over the Himalayas. Another study over the east and west coasts of India by Laskhmi &
116 Satyanarayana, (2020) discussed AR climatology and their impact on extreme precipitation. In these
117 studies, significant fraction (up to 40%) of extreme precipitation was observed to be associated with
118 ARs.

119 Above studies mainly focused on the southern India and did not identify ARs over the
120 Himalayas. However, as noted earlier, orographic barriers such as the Himalayas are the most
121 favorable locations where ARs exert pronounced impacts due to strong potential for vertical uplifting
122 of moisture (Hughes et al., 2014; Neiman et al., 2013; Rutz et al., 2014). In addition, a large population
123 (more than 1 billion) live in the Himalayan basins and are heavily dependent on glacier- and snow-fed
124 river systems for their municipal, hydropower, and agricultural water supplies.

125 ### 2.4 Objectives
126
127 The objective of this paper is to develop a dataset of ARs that penetrate the Himalayan transect.
128 The motivation of this work lies in the hypothesis that ARs exist and provide important contributions
129 to the water resources of the Himalayan basins. Though this has not been realized in the literature, we

https://doi.org/10.5194/essd-2020-397
Preprint. Discussion started: 19 February 2021


Open Access Earth System Science Data Discussions

believe that an easily accessible and freely available AR database can invigorate research on ARs and the Himalayan hydrology and will serve to advance the science of global ARs.

3 Study Area and Climate

The Himalayan mountain range, west to east extent, is ~2700 km long and has three major river basins i.e., Indus, Ganga, and Brahmaputra (Figure 1). These river basins cover an area of 2.75 million km^2 and contain some of the highly irrigated areas of the world with a total irrigated area of 577000 km^2 and the installed hydropower capacity of ~26000 MW.

Due to high altitudes and geographical location, the Himalayas together with Tibetan Plateau provides a physical barrier that plays key role in global weather patterns by acting as a heat source during the summer and a heat sink during the winter (Dimri et al., 2015). Climate of the Himalayas is complex because of the impact of two major circulation systems i.e. Indian summer monsoon and Western disturbances (Schiemann et al., 2008; Webster et al., 1998) (Figure 1). The Indian summer monsoon and WDs are associated with the movement of Intertropical Convergence Zone (ITCZ), which develops because of seasonal temperature and pressure differences between the northern and southern hemispheres (Gadgil and Joseph, 2003). During the summer season, Tibetan Plateau heats up and creates a void, to fill this void ISM originates from Indian Ocean, Arabian Sea and Bay of Bengal and move northward providing the maximum precipitation during June-September months (Maussion et al., 2014). Conversely, during winter season, Western Disturbances originate in the Mediterranean or West Atlantic region and travel across Iran, Iraq, Afghanistan, Pakistan and India and provide precipitation over the Himalaya (Rao et al., 1969).

The Indian summer monsoon intensity decreases from east to west while WDs weaken from west to east along the Himalayan range (Bookhagen and Burbank, 2006, 2010; Maussion et al., 2014). Besides, there are large differences in precipitation amounts across south-north axis of this mountain range because of its orography (Azam et al., 2014b; Maussion et al., 2014). The Himalayas act as a

https://doi.org/10.5194/essd-2020-397
Preprint. Discussion started: 19 February 2021


Open Access Earth System Science Data Discussions

barrier to the monsoon winds, causing huge orographic precipitation on the south slopes with a south-north gradient in the monsoon intensity (Dimri et al., 2015). Due to geographical location and regional orography, very wet regions coexist with very dry regions.

4 Data and Methods

4.1 Data

We use column integrated water vapor transport (IVT) to identify ARs, for which the required inputs are specific humidity and horizontal wind fields at multiple vertical levels of the troposphere. These fields are extracted from ECMWF's fifth generation reanalysis ERA5 (Hersbach et al., 2020) at 6-hourly temporal resolution, i.e., for each day, the fields are retrieved at four timesteps 00UTC, 06UTC, 12UTC, and 18UTC. ERA5 is improved with respect to its predecessor reanalysis data ERA-Interim through assimilating additional observational data and adopting new developments in physical modeling and data assimilation algorithms in its integrated forecasting system model. Significant improvements have been observed in simulating the atmospheric dynamics of the troposphere, which is where ARs are typically located; refer Hersbach et al., (2020) for details on ERA5 development. The data spans from the year 1979 to the present and covers the entire globe at a high horizontal resolution of 0.25°×0.25 (roughly 31km grid cell) at 137 vertical levels from the surface of earth.

The AR identification algorithm used in this study, discussed in next section, can at times confuse large-scale cyclones as ARs, and hence, these need to be removed before labeling the identified features as ARs. The dates and times of cyclones over the Bay of Bengal, Arabian Sea, and continental India are retrieved from the cyclone database maintained by the Regional Specialized Meteorological Centre (RSMC, www.rsmcnewdelhi.imd.gov.in), New Delhi, for tropical cyclones over the North India Ocean. The southern face of the Himalayas receive large amounts of orographic precipitation (Dimri et al., 2015; Maussion et al., 2014), which varies spatially and seasonally. Unfortunately, no satellite or reanalysis product is capable of capturing spatial variation and magnitude of precipitation over mountainous regions of the Himalayas (Andermann et al., 2012; Immerzeel et

https://doi.org/10.5194/essd-2020-397
Preprint. Discussion started: 19 February 2021

Open Access Earth System Science Data Discussions

al., 2015; Shen and Poulsen, 2018). Hence in this study, we use observation-based precipitation data provided by the India Metrological Department (IMD, Pai et al., (2014), www.imd.gov.in). Since large storms are normally expected during intense ARs, the concurrence of AR days with heavy precipitation from IMD will, to some extent, provide an independent verification of ARs identified in ERA5. The precipitation data is available at daily temporal and 0.25°×0.25° horizontal resolutions.

4.2 AR Identification

ARs are characterized by large moisture anomalies in the atmosphere, and since the availability of water vapor imagery from satellites, many studies used column integrated water vapor (IWV) observations from Special Sensor Microwave Imager/Sounder (SSM/I) to identify ARs (Neiman et al., 2008a, 2013; Ralph et al., 2004; Zhu and Newell, 1998).

Later, however, it was realized that IWV does not incorporate the flux component of ARs, and the column integrated water vapor transported (IVT), which includes horizontal winds in its computation, is taken as the preferred metric to identify ARs in most of the recent studies. IVT offers certain advantages over IWV in more coherently identifying ARs that show better relationship with precipitation and are more skillfully predicted by numerical weather prediction models (Cordeira et al., 2017; Dettinger et al., 2018; Nayak et al., 2014; Waliser and Guan, 2017; Young et al., 2017). IVT magnitude on a grid cell is computed as the magnitude of column integrated zonal and meridional moisture fluxes, as given in Equation 1 below.

$$IVT = g^{-1}\sqrt{\left(\int_{1000hPa}^{300hpa} qudp\right)^2 + \left(\int_{1000hPa}^{300hpa} qvdp\right)^2} \quad (1)$$

where, *IVT* is magnitude of water vapor transport in $kg.m^{-1}.s^{-1}$, q is specific humidity in $kg.kg^{-1}$, u and v are, respectively, zonal and meridional wind velocities in $m.s^{-1}$, and g is the acceleration due to gravity ($9.81ms^{-2}$).

https://doi.org/10.5194/essd-2020-397
Preprint. Discussion started: 19 February 2021


Open Access Earth System Science Data Discussions

Many algorithms are available to identify ARs using IVT fields (Lora et al., 2020; Shields et al., 2018); here, we use the algorithm developed by Lavers et al., (2012) for its conceptual and computational simplicity. The algorithm has been successfully employed in many AR studies over the US West Coast (Barth et al., 2017), Europe (Lavers &Villarini, 2015a, 2015b), and the central US (Lavers &Villarini, 2013a; Nayak et al., 2016; Nayak & Villarini, 2017).

[Step 1] The first step of the algorithm is to draw a geographical transect for the study region, and the ARs that penetrate it are selected as the ARs for the study area. For our study region, a transect based on ERA5 grid cells was selected at the southern front of the Himalayas as shown in Figure 1a. The transect (~1000 m a.s.l.) covers the entire arc of the Himalayas, except the elevated topography ahead and below the eastern and western Himalaya, respectively, since these will significantly reduce the lower-level moisture flow, which is a typical characteristic of ARs.

[Step 2] The next step is to find a threshold for IVT, above which an IVT field for any time instant may be considered a potential AR instant. As in many studies, the 85th percentile of daily IVT distribution is considered as the threshold. At each grid cell on the transect (Figure 1a), we take the 85th percentile of the daily IVT distributions, *i.e.*, 40 values for each day for the period 1979–2018. The daily thresholds are smoothed by taking a 15-day moving average centered on that day. Owing to latitudinal atmospheric temperature variations, the mean atmospheric water vapor and its flux varies latitudinally, decreasing northward, hence we considered latitudinally-varying thresholds. As can be noted, however, the transect is formed of numerous grid cells; thus, for simplicity, we divide the transect in five bins (from BinA for the eastern Himalaya to BinE for the western Himalaya), as shown in Figure 1a. For each bin, threshold for each day of year is taken as the average of the thresholds of the grid cells forming the bin. This way we construct daily- and latitudinally-varying IVT threshold series (Figure 1b).

[Step 3] The next step involves searching for a potential AR major axis from the IVT field at a given timestep. For the timestep, the maximum IVT grid cell among the grid cells of the entire

https://doi.org/10.5194/essd-2020-397
Preprint. Discussion started: 19 February 2021

transect is identified, and its IVT is compared with the threshold of the bin where the grid cell is located. This maximum IVT grid cell is taken as the first point of major axis for the potential AR timestep. As in Barth et al., (2017) taking the grid cell as the reference location, three grid cells on the next longitude eastwards are searched for the next point of the potential major axis. If the maximum IVT among the three grid cells is higher than the threshold, the new grid cell, where the IVT is highest, is saved as the second point of the major axis, and the search proceeds eastward from it. The search proceeds until either the IVT falls below the threshold or the length of the AR major axis is larger than $2000\ km$, at which point the timestep is considered as an AR timestep. Most studies take $2000\ km$ as the length criterion for identifying ARs (Fish et al., 2019; Guan and Waliser, 2015; Neiman et al., 2008b; Wick et al., 2013; Zhou et al., 2018) though smaller length criterion of 1500 km are also taken in some studies (Lakshmi and Satyanarayana, 2019; Lavers et al., 2013; Lavers and Villarini, 2013b; Ramos et al., 2016; Thapa et al., 2018). Similarly, a southward search is made, and the dates and time instances of all AR time steps identified are stored along with IVT values at grid cells of the major axes.

[Step 4] Tracking only along the longitudes (i.e., by searching only southward) and then only along the latitudes (*i.e.*, by searching only southward) allows us to identify only long rivers and remove most of the small-scale cyclonic structures. We also remove cyclones in RMSC database that are misidentified as potential AR timesteps. This is done by excluding all 6-hourly times of all cyclones, from genesis to termination, from the timesteps earlier identified as AR timesteps. Though ARs are often associated with cyclones, they are distinct from cyclones (Guan and Waliser, 2019; Pan and Lu, 2019), and it was deemed necessary to remove all cyclones regardless of the basin of origin, since all basins considered in RMSC database are in close proximity to the study region.

[Step 5] After removing cyclones from AR timesteps, 18-hour persistence criterion was adopted to exclude short-lived AR structures. From here onwards, we define an AR or AR-event as the one when AR conditions are met for a minimum of three consecutive six-hour timesteps (18-

https://doi.org/10.5194/essd-2020-397
Preprint. Discussion started: 19 February 2021


Open Access Earth System Science Data Discussions

257 hours), i.e., we only consider persistent ARs. The time for which AR conditions sustain is taken as the
258 duration of the AR. The 18-hour duration criterion is implemented in most studies on hydrologic
259 impacts of AR (Albano et al., 2020; Lakshmi and Satyanarayana, 2019), since ARs usually cause small
260 magnitude precipitation in the initial 18 hours (Ralph et al., 2019; Rutz et al., 2014)

261 The criteria of one-way searches, excluding cyclones, and 18-hour persistence are important,
262 since many large-diameter IVT "blobs", which would have otherwise been confused as ARs, are
263 removed. Over the eastmost Bin, BinE, a few ARs identified appear like "blobs" (not shown here)
264 may be due to elevated topography just south and east of the bin (Figure 1a), which diverts the ARs
265 from their expected trajectory towards the Himalayas. These are considered as ARs here, though it
266 might be more reasonable to exclude them from AR database.

267 [Step 6] Now, it is likely that many ARs identified in eastward search also appear in southward
268 search. In order to avoid double counting these ARs and to maintain their spatial and temporally
269 coherency, all ARs were merged to form a single AR database as follows. For ARs in which at least
270 one timestep overlapped in both searches, the AR for which average IVT magnitude (averaged taken
271 over the entire length and duration of AR) was greater was saved in the AR database, and the smaller-
272 IVT AR was discarded. ARs that did not overlap in the searches were concatenated to the database
273 without any change. The developed AR database in this study consists of dates and times of ARs, their
274 major axes, duration, and their intensities and categories as defined in the next section.

275 ### 4.3 AR Categorization

276 As seen in the literature, ARs produce diverse range of hydrometeorological impacts over
277 many regions of the globe; while many ARs supply beneficial water, some generate disastrous
278 precipitation. In an attempt to distinguish between beneficial and hazardous ARs for operational
279 purposes of weather prediction centers and water managers, Ralph et al., (2019) suggested a scale to
280 characterize ARs. The two most important factors that govern the strength and impact of an AR are
281 its IVT intensity and duration. It is noted that although IVT magnitude signifies an AR's impact in

https://doi.org/10.5194/essd-2020-397
Preprint. Discussion started: 19 February 2021

terms of rainfall intensities it generates, the duration mainly governs the storm-total precipitation and runoff variability (Lamjiri et al., 2017; Nayak et al., 2016; Ralph et al., 2013). Based on these considerations, Ralph et al., (2019) proposed AR categories (Cats) in their Table 2 and Figure 4, where ARs falling in Cat 1 to 2 are mostly beneficial, and those in 3 to 5 are hazardous, with 5 recognized as the most hazardous. Ralph et al., (2019) mainly focused on ARs landfalling over the US West Coast, where the IVT threshold to define an AR is $250\ kgm^{-1}s^{-1}$, and thus Cat 1 AR IVT intensity ranges from $250\ kgm^{-1}s^{-1}$ to $500\ kgm^{-1}s^{-1}$, Cat 2 ranges between $500\ kgm^{-1}s^{-1}$ to $750\ kgm^{-1}s^{-1}$, Cat 3 ranges between $750\ kgm^{-1}s^{-1}$ to $1000\ kgm^{-1}s^{-1}$, Cat 4 ranges between $1000\ kgm^{-1}s^{-1}$ to $1250\ kgm^{-1}s^{-1}$ and Cat 5 ranges from $1250\ kgm^{-1}s^{-1}$onwards.

However, we noted that the climate of the Himalayas is different, and as will be shown later, the threshold of IVT varies significantly with seasons, hence some region-specific modifications to the AR categorization are necessary. AR categories adopted here are presented in Table 1, where AR intensity is given by $IVT_{\max}$, which is defined as the maximum IVT at the first grid cells of the major axes of the AR timesteps, *i.e.*, maximum over the starting IVTs where the search begins in each timestep of the AR. This definition of AR intensity is consistent with that given in Ralph et al., 2019. The major difference in AR categorization here and in Ralph et al., (2019) is that, unlike here, the events in the first row of Table 1, where AR intensity is less than $250kgm^{-1}s^{-1}$(i.e., from threshold value to $250kgm^{-1}s^{-1}$), are not considered as ARs in Ralph et al., (2019). Indeed, this categorization is not definitive and future research will elucidate the strengths and impacts of ARs over the Himalayas, and it will help in developing more precise operational categorization. As a starting point, however, the categorization in Table 1 can be taken as basis for understanding the climatology and impacts of weak and strong ARs.

Table 1: AR categorization based on AR Intensity ($\boldsymbol{IVT_{max}}$) and duration. Six AR categories are defined, with categories Cat 0 to Cat 2 taken as primarily beneficial and Cat 3 to Cat 5 are taken as primarily hazardous, as in Ralph et al., (2019).

https://doi.org/10.5194/essd-2020-397
Preprint. Discussion started: 19 February 2021

Open Access Earth System Science Data Discussions

IVT_{max} $(kgm^{-1}s^{-1})$	AR Duration (hours)		
	$<= 24$	$24-48$	>48
≤ 250	0	1	2
$>250-500$	1	2	3
$>500-750$	2	3	4
$>750-1000$	3	4	5
$>1000-1250$	4	5	5
>1250	5	5	5

4.4 AR tracks

The database developed in this study also provides the major axes of ARs, which can be loosely taken as the trajectories or tracks of ARs. The tracks of ARs provide critical information regarding their origin, moisture sources, and seasonal variability. As defined earlier (section 4.2), the major axis of an AR timestep is the collection of grid cells over which IVT is maximum. ARs are not stationary; the AR major axis changes from one timestep to the next. We collect all the major axes of an AR event and define the average of those axes as the track of the AR. Most AR timesteps have lengths more than the required $2000km$; here we show average over the length of the shortest major axis. For each season, we show tracks of 25 random ARs to give an overall picture of their likely trajectories in different seasons. The detailed analyses of moisture sources and trajectories of ARs is out of scope of the present study and is left for future studies.

5 Results and Discussion

5.1 AR events, frequency and trends

IVT threshold varies significantly with seasons and across latitudes (Figure 1b). The lowest values are observed in winter, following which the threshold rises abruptly in the Ganga Basin (within

https://doi.org/10.5194/essd-2020-397
Preprint. Discussion started: 19 February 2021

30 days the threshold increased from $200kgm^{-1}s^{-1}$ to $500kgm^{-1}s^{-1}$ in the southernmost bin, Bin E, peaking in summer and then again dropping towards the end of autumn (Figure 1b). The peak IVT in summer can likely be attributed to the Indian summer monsoon circulation, though it can be noticed that seasonal variation is less pronounced in the Indus Basin transects, bins A and B, which suggests that the Indus Basin is not heavily influenced by the monsoon. The monsoon reach and intensity over the Himalayas is also reflected in the large differences of summer thresholds across the bins; the smaller differences in winter, on the other hand, may be due to small south-north variations of air temperature and atmospheric moisture. Unlike a fixed threshold of $200kgm^{-1}s^{-1}$ used in most AR studies (Hecht and Cordeira, 2017; Lavers et al., 2012; Leung and Qian, 2009) the seasonally-varying threshold used here is aimed at extracting ARs from the background monsoon, due to which the normal IVT over the Himalayas is significantly higher than $200kgm^{-1}s^{-1}$ in summer (Figure 1b).

https://doi.org/10.5194/essd-2020-397
Preprint. Discussion started: 19 February 2021

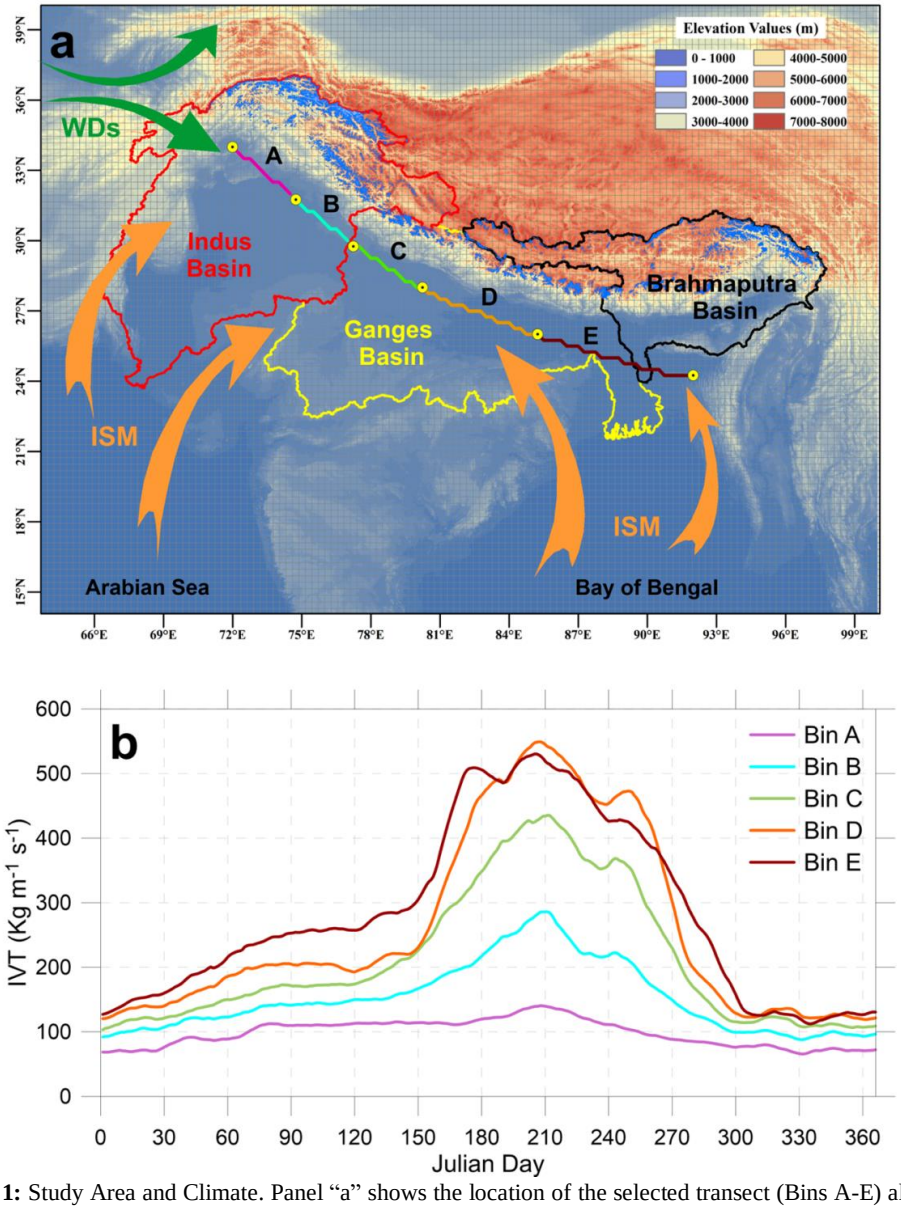

Figure 1: Study Area and Climate. Panel "a" shows the location of the selected transect (Bins A-E) along the Himalayan front (~1000 m.a.s.l.). Orange and green arrows show the major circulations affecting the region, the Indian summer monsoon and the western disturbances, respectively. The dark blue color in Indus, Ganges and Brahmaputra basins shows the glacierized area from GAMDAM inventory *(Nuimura et al., 2015)*. Background gridlines show the ERA5 horizontal grid spacing. Panel "b" shows the daily-varying 85th percentile of IVT distribution along the bins. See Data and Methods section for more details.

The frequency of ARs varies annually and marginally across seasons, with annual average of 23 and seasonal averages of 7, 5, 6, and 5 ARs in winter (December–February), spring (March–May),

https://doi.org/10.5194/essd-2020-397
Preprint. Discussion started: 19 February 2021

summer (June–August), and autumn (September–November), respectively (Figure 2a). The minimum ARs of 15 were found in 1987 while the maximum of 37 in 2006. The year-to-year variability in annual frequency marginally displays an oscillation of period roughly 3 to 4 years, which may be related to large scale climatic patterns (Collow et al., 2020). It can be noticed that over the 1990s, the frequency of ARs was consistently higher than the average frequency (Figure 2a).

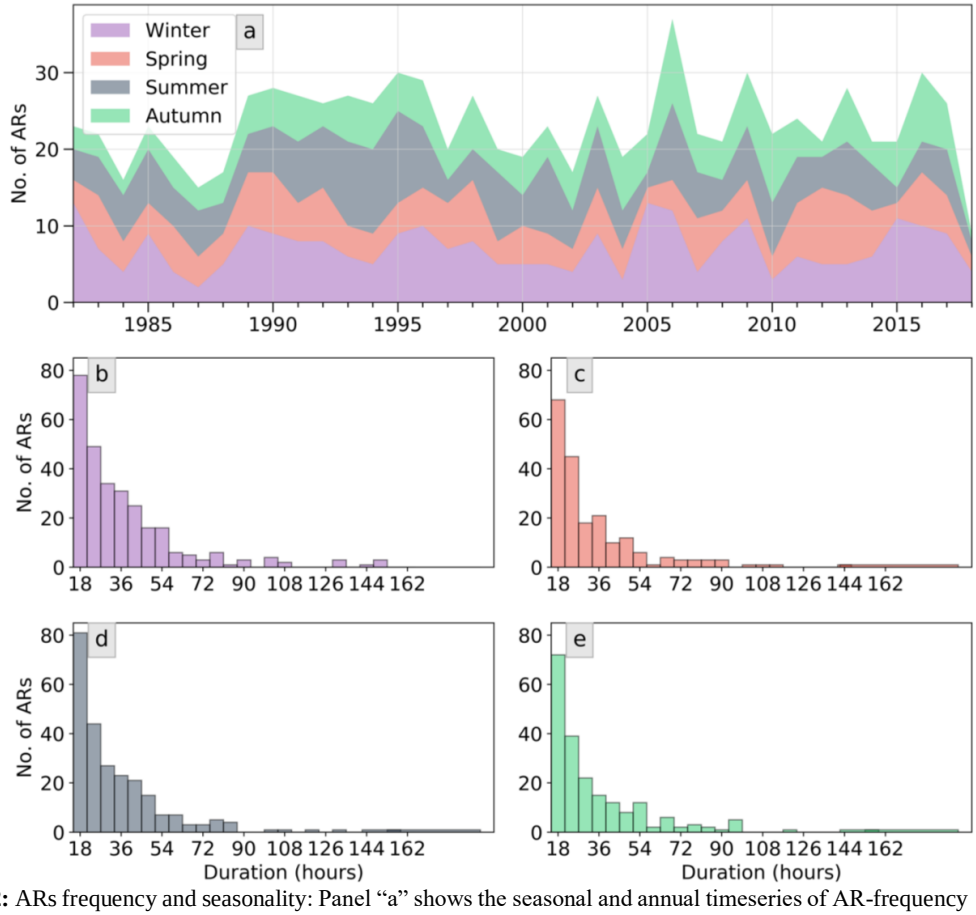

Figure 2: ARs frequency and seasonality: Panel "a" shows the seasonal and annual timeseries of AR-frequency over the Himalayas. Panels "b–d" show the distribution of duration of ARs in different seasons.

For discovering any temporal trends, the AR frequency of the four seasons is regressed on time (year) as an independent variable. The regression analysis yielded slopes close to zero for winter and spring seasons (p −values for slopes close to 0.8, which implies that the null hypothesis of no temporal trends cannot be rejected; see Figure S1 in Supplemental Material). However, a decreasing trend (-0.5

https://doi.org/10.5194/essd-2020-397
Preprint. Discussion started: 19 February 2021

ARs per decade, $p-value \cong 0.25$) and an increasing trend (+0.7 ARs per decade, $p-value \cong 0.04$, i.e., significant at 5% level) in summer and autumn frequencies of ARs are observed respectively. The decline in summer ARs may be linked to the weakening of summer monsoon highlighted in some recent studies (Mishra et al., 2012; Paul et al., 2016). This, however, would suggest that observed weakening of summer monsoon maybe in fact weakening of summer ARs, and the monsoon itself may not be weakening. More in-depth studies on trends in AR frequency of autumn and summer, and its links with the monsoon weakening may bring some interesting insights into light.

The duration of most ARs (more than 90%) is less than three days (Figure 2b-e); however, long-duration ARs that last for more than 72 hours (3 days), are also observed in all seasons. Winter ARs are in general longer lasting (median duration 30 hours) than those in other seasons, for which the median duration 24 hours.

Figure 3 shows the seasonal and category-wise distribution of ARs across the transect. It can be seen that winter is the most prominent season for AR occurrences across the Himalayas, except for the eastern Himalaya BinE (Figure 3). The higher frequency in winter can be related to increased meridional tropospheric temperature gradient, where baroclinic instability increases the likelihood of cyclone formation and WDs (Hunt et al., 2018b; Rao et al., 1971). Only a few ARs are observed over BinA in summer, which again suggests that the Indian Summer Monsoon has little effect on the climate of the Indus Basin. In contrast, the southernmost transect BinE experiences the highest frequency of ARs in summer, which suggests that most ARs over the eastern Ganga Basin are linked to the Indian Summer Monsoon. Except for extreme Bins (BinA and BinE), all the other bins have nearly uniform frequency of ARs in spring, summer and autumn (Figure 3).

https://doi.org/10.5194/essd-2020-397
Preprint. Discussion started: 19 February 2021

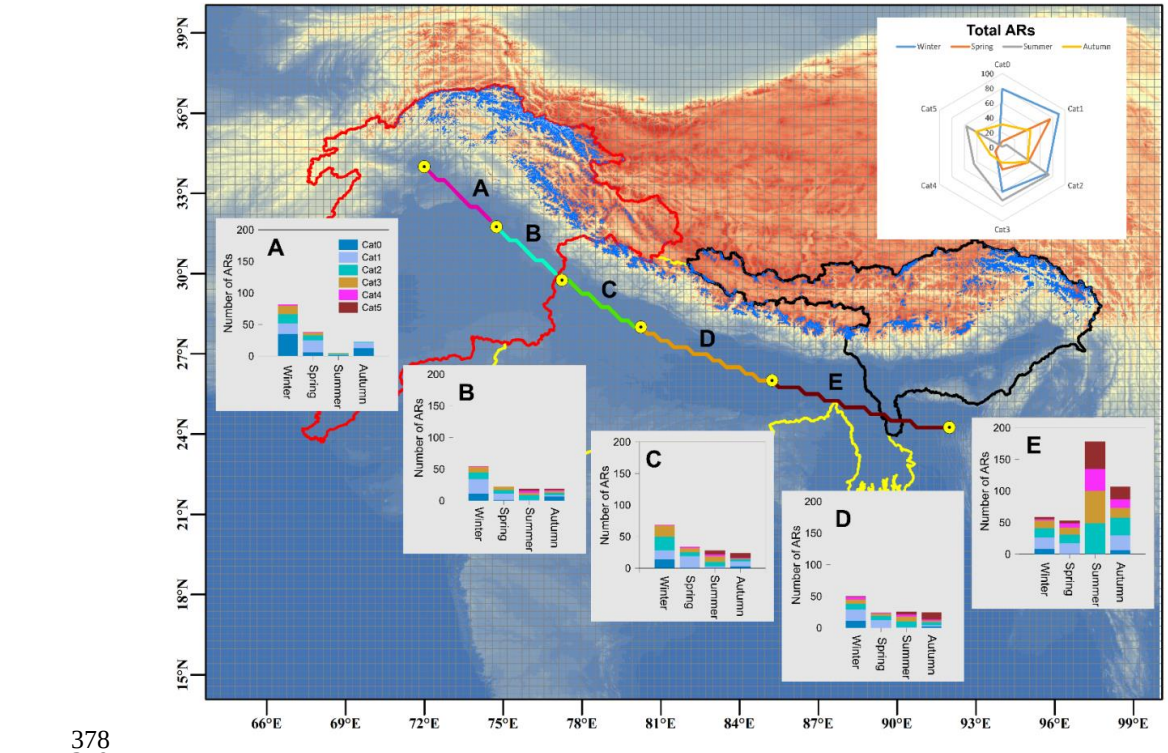

Figure 3: ARs Categories: Panel "A–E" show the distribution of ARs categories in different seasons over the five bins (A to E) along the transect. The inset shows the fractional distribution of AR categories in different seasons.

Most ARs that penetrate the Indus Basin are of weak categories 0 and 1, with only a few falling in disaster categories Cat 4 and 5; in fact, no Cat 5 AR is observed in western Indus BinA. For the eastern Ganga and Brahmaputra basins (BinE), majority of ARs are of Cat 3 or higher, since most of them happened in the monsoon season when the moisture transport in the atmosphere is in general large (Bookhagen and Burbank, 2006; Maussion et al., 2014). These higher category ARs over Bin E are most probably the reason for the frequent flooding in Nepal, NE India, and Bangladesh (Thapa et al., 2018; Yang et al., 2018). The radar diagram (inset in Figure 3) suggests that a large faction of ARs in summer are Cat 3 and higher, where for other seasons, majority of ARs are of Cat 3 or lower, i.e., mostly beneficial.

https://doi.org/10.5194/essd-2020-397
Preprint. Discussion started: 19 February 2021

5.2 AR tracks

The major axes of 25 random ARs in each season, and each axis is averaged over the AR's life span, are plotted as lines in Figure 4; these lines thus represent the typical tracks of ARs in different seasons. From these tracks, we observe that majority of the ARs in winter and spring travel (the word *travel* is used loosely here to indicate axis of AR moisture transport) over the northern extremities of the Arabian Sea (Figure 4). Due to higher baroclinic instability, winter and spring are favorable seasons for the occurrences of WDs, which are extratropical cyclonic systems that generally originate in the Mediterranean region and are embedded in and moved eastwards by the subtropical westerly jet (SWJ) stream (Dimri and Chevuturi, 2016; Hunt et al., 2018a). These systems are known to bring moisture from the surrounding seas (Bookhagen and Burbank, 2006), mostly from the Mediterranean Sea and the Atlantic Ocean, more accurate estimates of major moisture sources of the ARs, however, can be obtained from Lagrangian trajectory analyses (Nayak et al., 2016; Sodemann and Stohl, 2013). As discussed in the introduction section, the presence of cyclonic systems and jet streams are typical features of ARs. In addition, the poleward component of moisture transport, a typical feature of ARs, is apparent in ARs of all seasons (Figure 4).

WDs and SWJ are mostly absent during summer and autumn and only limited number of ARs travel over the northern Arabian Sea. Most ARs in these seasons travel over the southern Arabian sea and the Bay of Bengal, and their tracks indicate that they may be associated with the Indian Summer Monsoon and systems affecting it, such as the Somali Jet, ITCZ, Tropical Easterly Jet. A detailed association of ARs in summer with the monsoon circulation is a subject for future investigation.

From Figure 4, we also observed ARs that travelled over the northern Arabian Sea are generally of weak categories, and, in contrast, the ARs that travelled over the Bay of Bengal fall generally in strong categories, stronger than Cat 3. This is most likely because ARs over the Bay of Bengal travel over the tropics, where atmosphere is generally hot and humid as compared to northern Arabian sea. Interestingly, it is noticed that the Bay of Bengal ARs mostly have confined region of travel, landfall

https://doi.org/10.5194/essd-2020-397
Preprint. Discussion started: 19 February 2021

exclusively over the southern bins of the transect, and rarely travel to the Indus and northern Ganga basins. These traits can be relevant in forecasting ARs and their impacts over the Himalayas.

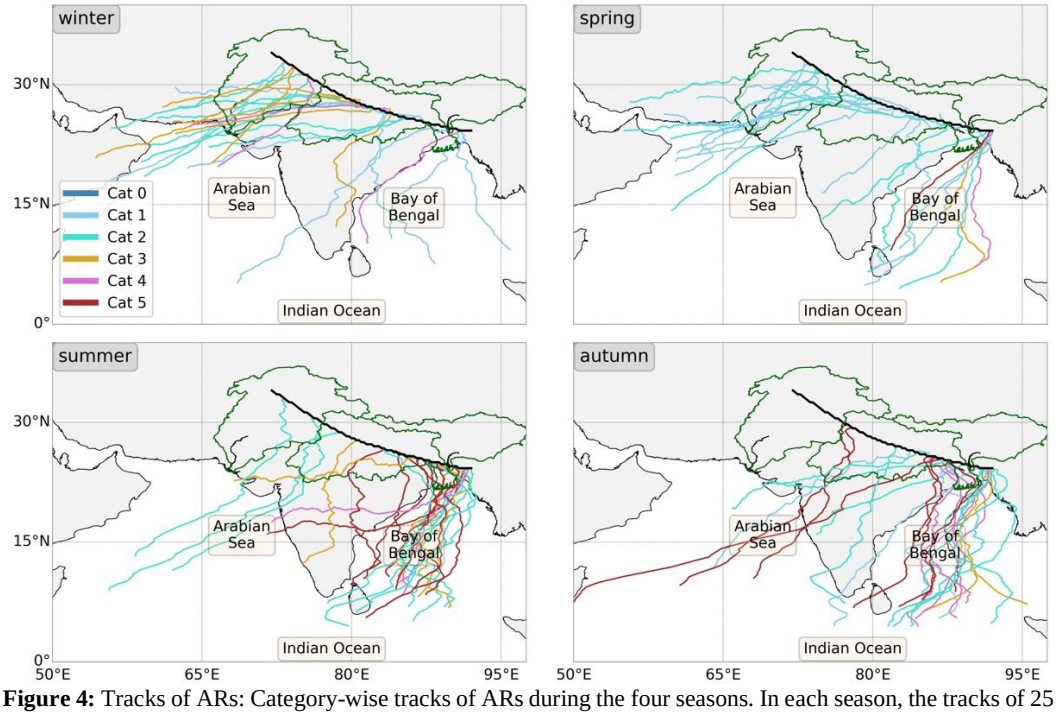

Figure 4: Tracks of ARs: Category-wise tracks of ARs during the four seasons. In each season, the tracks of 25 randomly selected ARs are drawn to show the favored paths of ARs. Here, an AR-track is defined as the major axis of the AR, see text for more details.

5.3 Precipitation Impacts

The primary goal of this paper is to develop an AR database over the Himalayas; however, it is important to see whether or not, and to what extent, ARs impact the hydrology of the Himalayan rivers basins, as they do in other mountainous regions. ARs impact the hydrology of a basin primarily through the precipitation that is generated when the moisture-laden air is lifted by orography or other dynamical mechanisms, such as frontal lifting. The purpose of this section is to provide a brief overview of the impacts ARs can have on the precipitation over the Himalayas, so that their contribution in shaping the hydrology of the basins may be appreciated in the scientific literature. Figure 5 shows the observation-based daily precipitation intensities from IMD corresponding to four

https://doi.org/10.5194/essd-2020-397
Preprint. Discussion started: 19 February 2021

long-duration (duration of at least 3 days) and highest intensity ARs, two over each the Indus and the Ganga basins which span the entire transect of our analysis. In all the four ARs, long and relatively narrow bands of intense moisture transports are observed over the northern and southern Arabian Sea. The ARs dumped large quantities of moisture as precipitation along their tracks over the plains and near the foothills of Himalayas and higher elevations, upon confronting the Himalayan topographic barrier (represented by the transect in Figure 5). It can be assumed with some certainty that the topographic barrier vertically lifted the moisture in the ARs, resulting in intense orographic precipitation. From panels b2 and c2 of Figure 5, we observed that the heavy precipitation events associated with ARs can occur over higher altitude (4000–5000 m.a.sl.) glacierized regions. ARs, in general, are warmer than the ambient atmosphere; in this perspective, these results can have profound impacts on the mass balance and health of glaciers over the Himalayas, which will be discussed further in the final section.

https://doi.org/10.5194/essd-2020-397
Preprint. Discussion started: 19 February 2021

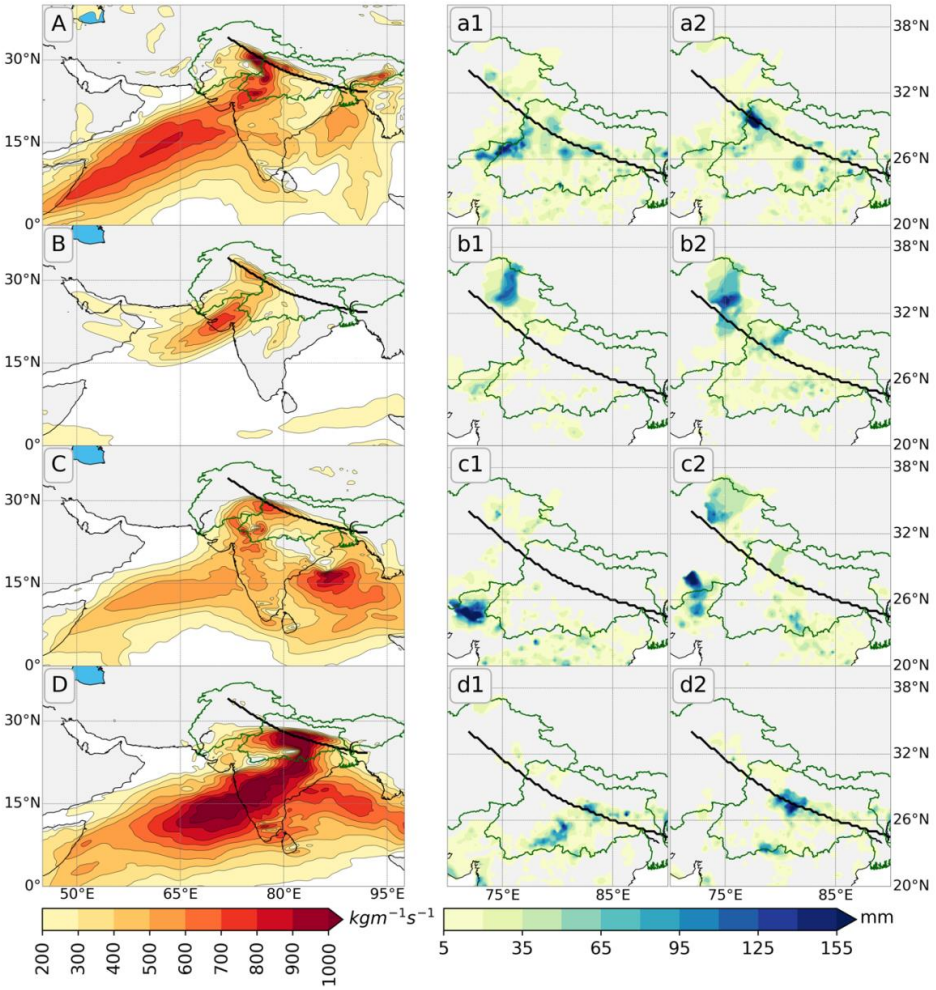

Figure 5: Precipitation impacts of ARs: Left panels show IVT fields of the two highest-intensity long-duration ($duration \geq 3\ days$) ARs over the Indus basin (panel "A" for AR at 1983-07-25 18UTC and panel "B" for AR at 2003-02-16 06UTC) and over the Ganga basin (panel "C" for AR at 1992-09-06 12UTC, and panel "D" for AR at 2007-09-21 00UTC). The right panels show the corresponding daily precipitation amounts from IMD on the second and third day of the AR incidence.

To appreciate the intensity of AR-induced precipitation in a climatological perspective, we first note that over the Himalayas, the 95th percentile of daily precipitation distribution based on wet days (defined as days with precipitation larger than 2mm) is roughly 70mm, and the 99th percentile ranges from 90mm to 125mm. In the right panels of Figure 5, we see that the precipitation intensity associated with four ARs is larger than 150mm per day, i.e., much higher than the 99th percentile over a large area, and heavy precipitation crossing the 95th percentile is widespread over thousands of

https://doi.org/10.5194/essd-2020-397
Preprint. Discussion started: 19 February 2021


Open Access Earth System Science Data Discussions

456 square kilometers. Such large intensities of precipitation persistently for multiple AR days may
457 contribute a substantial fraction to the annual accumulated precipitation over the basins. From the
458 figure, it can also be observed that ARs reach higher altitudes ($> 4000\, m.a.s.l$), where they may
459 result in severe snowstorms and affect the snow-mass balance of the regions.

460 We inspected additional six high-intensity ARs in each basin (shown in supplementary
461 material Figures S2–S3); in majority of them (9 out of 12), widespread heavy precipitation days are
462 observed. These results indicate that ARs have significant impacts on the water availability, flooding
463 risks, and glacier health over the Himalayas. Detailed investigations into the hydrological and
464 ecological impacts of ARs over the Himalayas are left for future studies.

465 6 Conclusions and Future Prospective

466 In the present study, for the first time, we constructed a ready-to-use database of ARs over the
467 Himalayas using ERA5 atmospheric fields since 1982. We used a seasonally varying threshold of IVT
468 along the Himalayan front in order to extract the ARs. The extracted ARs were further investigated
469 for their timing, frequency, duration, seasonality, tracks, and trends. The annual frequency of ARs
470 varied from 15 in 1987 to 35 in 2006 with an average of 23 over 1982–2018 period. The duration of
471 most ARs (~90%) was less than 3 days, though longer-duration AR are not uncommon. AR occurrence
472 was most frequent during winter over most of the Himalayan region, except for eastern Ganga and
473 Brahmaputra basins where highest frequency was observed during summer, which may be linked with
474 highest summer monsoon activity. We categorized the ARs in six categories, ranging from beneficial
475 to the most hazardous, based on their intensity and duration. ARs over the Indus Basin, mainly travel
476 through the Arabian Sea, were mostly of beneficial categories (Cats 0–2), while ARs over the eastern
477 Ganga and Brahmaputra basins, mainly travel through the Bay of Bengal, were often hazardous
478 categories (Cats 3–5).

479 ARs, extreme precipitations, and floods: Recently ARs have been discussed widely for their
480 societal impacts linked with extreme precipitation in many mountainous regions around the world.

https://doi.org/10.5194/essd-2020-397
Preprint. Discussion started: 19 February 2021

Unfortunately, ARs have been poorly investigated over the Himalayas and consequently the linkages between ARs and Himalayan hydrology as well as extreme precipitation events are not studied yet. However, in this study a preliminary investigation between observed ARs and IMD field-based gridded precipitation data clearly established that ARs are tightly associated with widespread heavy precipitation days over the Himalayas and can deliver precipitation intensities as high as 150 mm per day. Though some recent studies effectively linked individual flooding in south India with ARs (Lakshmi et al., 2019; Laskhmi and Satyanarayana, 2020; Liang and Yong, 2020), but such studies are scarce over the Himalayan region (Thapa et al., 2018). Our analysis (section 5.3) indicates a strong association of frequent flooding over the eastern Ganga and Brahmaputra basins with ARs, though further research is needed to ascertain the association. Recent flood hazards in the Himalayan region including cloud burst flood in Leh in August 2010 (Dimri et al., 2017), Kedarnath flood in June 2013(Bhambri et al., 2016) and Kashmir flood in September 2014 (Romshoo et al., 2018) have been discussed as a result of extreme precipitation events but potential linkages of these floods with ARs have not been explored yet.

ARs and precipitation trends: While the climate warming is unequivocal, long-term precipitation does not show any particular trend over the past decades in the Himalayan region (Krishnan et al., 2019). The frequency of ARs over the Himalayas did not show any significant trend in winter and spring seasons; increasing and decreasing trends, however, are observed in autumn and summer monsoon seasons, respectively. In northern India, the observed reduced annual precipitations were thought to be due to weakening of the Indian summer monsoon since 1950s (Mishra et al., 2012; Paul et al., 2016). We conjecture that the reducing annual precipitations may be associated with decreasing ARs during the summer monsoon. However, dedicated studies investigating the ARs and monsoon weakening over the Himalayan region can bring some concrete conclusions on this perspective.

ARs and the Himalayan cryosphere: The Himalayan glaciers are exposed to different climatic conditions from west to east depending on their geographical location (Maussion et al., 2014).

https://doi.org/10.5194/essd-2020-397
Preprint. Discussion started: 19 February 2021


Open Access Earth System Science Data Discussions

Numerous field- or model-based studies in the Himalayas advocated that while the combined annual snow accumulation from the Indian summer monsoon and Western Disturbances shape the glacier mass balances, it is mainly governed by the snow conditions during the summer monsoon (Azam et al., 2014a, 2014b; Fujita, 2008; Mandal et al., 2020). Therefore the timing and amount of snowfall during the melt season are critical factors for the surface energy balance of the Himalayan glaciers, irrespective of their geographical location. Heavy snowfalls, controlling the glacier mass balances and meltwater, were simply thought to be rooted in summer-monsoon circulation (Azam et al., 2014b; Fujita, 2008; Maussion et al., 2014; Mölg et al., 2014). Our study clearly showed ARs' reach to higher altitudes (up to 4000-5000 m a.s.l.; Figure 5 and Supplementary Figures S2–S3), and we inferr that due to lower temperatures at higher elevations, ARs have potential to the deliver heavy snowfalls on the glaciers. Strong snowfalls associated with multiple-day ARs can abruptly change the surface energy balance on glaciers by increasing surface albedo, especially in the summer melting period, and thus might be a major driver for glacier mass balance in the Himalayas.

Detailed investigation of the impact of ARs on the Himalayan water resources is beyond the scope of the present study. Nevertheless, some inferences in our study from the AR dataset developed offer new lines of research in the Himalayas and invite researchers to investigate the control of ARs on the health of glaciers, generated melt waters, extreme precipitations, flooding and rain-on-snow events in the Himalayan basins.

Data Availability

The data is available at Zenodo repository at https://doi.org/10.5281/zenodo.4451901 (Nayak et al., 2021). We have also included the data in our Supplementary Information file.

Acknowledgement

Munir Ahmad Nayak and Rosa Vellosa Lyngwa gratefully acknowledge the financial support provided by the Science and Engineering Research Board (SERB) of the Department of Science and Technology

https://doi.org/10.5194/essd-2020-397
Preprint. Discussion started: 19 February 2021

(DST), Government of India, under the Early Career Research (ECR) award ECR/2017/002782. We acknowledge and thank European Centre for Medium-Range Weather Forecasts (ECMWF) for keeping the data publicly accessible, without which the study would not have been possible.

The authors declare no competing interests.

References

Albano, C. M., Dettinger, M. D. and Harpold, A. A.: Patterns and drivers of Atmospheric River precipitation and hydrologic impacts across the Western United States, J. Hydrometeorol., 21(1), 143–159, doi:10.1175/JHM-D-19-0119.1, 2020.

Andermann, C., Longuevergne, L., Bonnet, S., Crave, A., Davy, P. and Gloaguen, R.: Impact of transient groundwater storage on the discharge of Himalayan rivers, Nat. Geosci., 5(2), 127–132, doi:10.1038/ngeo1356, 2012.

Azam, M. F., Wagnon, P., Vincent, C., Ramanathan, A., Favier, V., Mandal, A. and Pottakkal, J. G.: Processes governing the mass balance of Chhota Shigri Glacier (western Himalaya, India) assessed by point-scale surface energy balance measurements, The Cryosphere, 8(6), 2195–2217, doi:10.5194/tc-8-2195-2014, 2014a.

Azam, M. F., Wagnon, P., Vincent, C., Ramanathan, A., Linda, A. and Singh, V. B.: Reconstruction of the annual mass balance of Chhota Shigri glacier, Western Himalaya, India, since 1969, Ann. Glaciol., 55(66), 69–80, doi:10.3189/2014AoG66A104, 2014b.

Azam, M. F., Wagnon, P., Berthier, E., Vincent, C., Fujita, K. and Kargel, J. S.: Review of the status and mass changes of Himalayan-Karakoram glaciers, J. Glaciol., 64(243), 61–74, doi:10.1017/jog.2017.86, 2018.

Banerjee, A. and Azam, M. F.: Temperature reconstruction from glacier length fluctuations in the Himalaya, Ann. Glaciol., 57(71), 189–198, doi:10.3189/2016AoG71A047, 2016.

Barth, N. A., Villarini, G., Nayak, M. A. and White, K.: Mixed populations and annual flood frequency estimates in the western United States: The role of atmospheric rivers: Atmosopheric rivers and west United States floods., Water Resour. Res., 53(1), 257–269, doi:10.1002/2016WR019064, 2017.

Bhambri, R., Mehta, M., Dobhal, D. P., Gupta, A. K., Pratap, B., Kesarwani, K. and Verma, A.: Devastation in the Kedarnath (Mandakini) Valley, Garhwal Himalaya, during 16–17 June 2013: a remote sensing and ground-based assessment, Nat. Hazards, 80(3), 1801–1822, doi:10.1007/s11069-015-2033-y, 2016.

Bhambri, R., Watson, C. S., Hewitt, K., Haritashya, U. K., Kargel, J. S., Pratap Shahi, A., Chand, P., Kumar, A., Verma, A. and Govil, H.: The hazardous 2017–2019 surge and river damming by Shispare Glacier, Karakoram, Sci. Rep., 10(1), 4685, doi:10.1038/s41598-020-61277-8, 2020.

Biemans, H., Siderius, C., Lutz, A. F., Nepal, S., Ahmad, B., Hassan, T., von Bloh, W., Wijngaard, R. R., Wester, P., Shrestha, A. B. and Immerzeel, W. W.: Importance of snow and glacier meltwater

https://doi.org/10.5194/essd-2020-397
Preprint. Discussion started: 19 February 2021

568 for agriculture on the Indo-Gangetic Plain, Nat. Sustain., 2(7), 594–601, doi:10.1038/s41893-019-
569 0305-3, 2019.

570 Bolch, T., Shea, J. M., Liu, S., Azam, F. M., Gao, Y., Gruber, S., Immerzeel, W. W., Kulkarni, A.,
571 Li, H., Tahir, A. A., Zhang, G. and Zhang, Y.: Status and change of the cryosphere in the extended
572 Hindu Kush Himalaya Region, in The Hindu Kush Himalaya Assessment, edited by P. Wester, A.
573 Mishra, A. Mukherji, and A. B. Shrestha, pp. 209–255, Springer International Publishing, Cham.,
574 2019.

575 Bookhagen, B. and Burbank, D. W.: Topography, relief, and TRMM-derived rainfall variations
576 along the Himalaya, Geophys. Res. Lett., 33(8), L08405, doi:10.1029/2006GL026037, 2006.

577 Bookhagen, B. and Burbank, D. W.: Toward a complete Himalayan hydrological budget:
578 Spatiotemporal distribution of snowmelt and rainfall and their impact on river discharge, J. Geophys.
579 Res., 115(F3), F03019, doi:10.1029/2009JF001426, 2010.

580 Brun, F., Berthier, E., Wagnon, P., Kääb, A. and Treichler, D.: A spatially resolved estimate of high
581 mountain Asia glacier mass balances from 2000 to 2016, Nat. Geosci., 10(9), 668–673,
582 doi:http://dx.doi.org/10.1038/ngeo2999, 2018.

583 Chen, X., Leung, L. R., Wigmosta, M. and Richmond, M.: Impact of atmospheric rivers on surface
584 hydrological processes in western U.S. watersheds, J. Geophys. Res. Atmospheres, 124(16), 8896–
585 8916, doi:10.1029/2019JD030468, 2019.

586 Collow, A. B. M., Mersiovsky, H. and Bosilovich, M. G.: Large-scale influences on Atmospheric
587 River–induced extreme precipitation events along the Coast of Washington State, J. Hydrometeorol.,
588 21(9), 2139–2156, doi:10.1175/JHM-D-19-0272.1, 2020.

589 Cordeira, J. M., Ralph, F. M. and Moore, B. J.: The development and evolution of two Atmospheric
590 rivers in proximity to Western North Pacific Tropical Cyclones in October 2010, Mon. Weather
591 Rev., 141(12), 4234–4255, doi:10.1175/MWR-D-13-00019.1, 2013.

592 Cordeira, J. M., Ralph, F. M., Martin, A., Gaggini, N., Spackman, J. R., Neiman, P. J., Rutz, J. J. and
593 Pierce, R.: Forecasting Atmospheric rivers during CalWater 2015, Bull. Am. Meteorol. Soc., 98(3),
594 449–459, doi:10.1175/BAMS-D-15-00245.1, 2017.

595 Dettinger, M. D. and Cayan, D. R.: Drought and the California delta—A matter of extremes, San
596 Franc. Estuary Watershed Sci., 12(2), doi:10.15447/sfews.2014v12iss2art4, 2014.

597 Dettinger, M. D., Ralph, F. M., Das, T., Neiman, P. J. and Cayan, D. R.: Atmospheric rivers, floods
598 and the water resources of California, Water, 3(2), 445–478, doi:10.3390/w3020445, 2011.

599 Dettinger, M. D., Ralph, F. M. and Rutz, J. J.: Empirical Return Periods of the Most Intense Vapor
600 Transports during Historical Atmospheric River Landfalls on the U.S. West Coast, J.
601 Hydrometeorol., 19(8), 1363–1377, doi:10.1175/JHM-D-17-0247.1, 2018.

602 Dimri, A. P. and Chevuturi, A.: Western Disturbances - An Indian Meteorological perspective,
603 Springer International Publishing, Cham., 2016.

604 Dimri, A. P., Niyogi, D., Barros, A. P., Ridley, J., Mohanty, U. C., Yasunari, T. and Sikka, D. R.:
605 Western Disturbances: A review, Rev. Geophys., 53(2), 225–246, doi:10.1002/2014RG000460,
606 2015.

https://doi.org/10.5194/essd-2020-397
Preprint. Discussion started: 19 February 2021

607 Dimri, A. P., Chevuturi, A., Niyogi, D., Thayyen, R. J., Ray, K., Tripathi, S. N., Pandey, A. K. and
608 Mohanty, U. C.: Cloudbursts in Indian Himalayas: A review, Earth-Sci. Rev., 168, 1–23,
609 doi:10.1016/j.earscirev.2017.03.006, 2017.

610 Farinotti, D., Huss, M., Fürst, J. J., Landmann, J., Machguth, H., Maussion, F. and Pandit, A.: A
611 consensus estimate for the ice thickness distribution of all glaciers on Earth, Nat. Geosci., 12(3),
612 168–173, doi:10.1038/s41561-019-0300-3, 2019.

613 Fish, M. A., Wilson, A. M. and Ralph, F. M.: Atmospheric river families: Definition and associated
614 synoptic conditions, J. Hydrometeorol., 20(10), 2091–2108, doi:10.1175/JHM-D-18-0217.1, 2019.

615 Florsheim, J. L. and Dettinger, M. D.: Promoting Atmospheric-river and snowmelt-fueled
616 biogeomorphic processes by restoring river-floodplain connectivity in California's Central Valley, in
617 Geomorphic Approaches to Integrated Floodplain Management of Lowland Fluvial Systems in North
618 America and Europe, edited by P. F. Hudson and H. Middelkoop, pp. 119–141, Springer New York,
619 New York, NY., 2015.

620 Fujita, K.: Effect of precipitation seasonality on climatic sensitivity of glacier mass balance, Earth
621 Planet. Sci. Lett., 276(1–2), 14–19, doi:10.1016/j.epsl.2008.08.028, 2008.

622 Gadgil, S. and Joseph, P. V.: On breaks of the Indian monsoon, J. Earth Syst. Sci., 112(4), 529–558,
623 doi:10.1007/BF02709778, 2003.

624 Guan, B. and Chan, J. C. L.: Nonstationarity of the Intraseasonal Oscillations Associated with the
625 Western North Pacific Summer Monsoon, J. Clim., 19(4), 622–629, doi:10.1175/JCLI3661.1, 2006.

626 Guan, B. and Waliser, D. E.: Detection of atmospheric rivers: Evaluation and application of an
627 algorithm for global studies, J. Geophys. Res. Atmospheres, 120(24), 12514–12535,
628 doi:10.1002/2015JD024257, 2015.

629 Guan, B. and Waliser, D. E.: Tracking Atmospheric rivers globally: Spatial distributions and
630 temporal evolution of life cycle characteristics, J. Geophys. Res. Atmospheres, 124(23), 12523–
631 12552, doi:10.1029/2019JD031205, 2019.

632 Guan, B., Molotch, N. P., Waliser, D. E., Fetzer, E. J. and Neiman, P. J.: Extreme snowfall events
633 linked to atmospheric rivers and surface air temperature via satellite measurements, Geophys. Res.
634 Lett., 37(20), doi:https://doi.org/10.1029/2010GL044696, 2010.

635 Hecht, C. W. and Cordeira, J. M.: Characterizing the influence of atmospheric river orientation and
636 intensity on precipitation distributions over North Coastal California: ARs and Precipitation Over
637 North Coastal CA, Geophys. Res. Lett., 44(17), 9048–9058, doi:10.1002/2017GL074179, 2017.

638 Hersbach, H., Bell, B., Berrisford, P., Hirahara, S., Horányi, A., Muñoz-Sabater, J., Nicolas, J.,
639 Peubey, C., Radu, R., Schepers, D., Simmons, A., Soci, C., Abdalla, S., Abellan, X., Balsamo, G.,
640 Bechtold, P., Biavati, G., Bidlot, J., Bonavita, M., Chiara, G., Dahlgren, P., Dee, D., Diamantakis,
641 M., Dragani, R., Flemming, J., Forbes, R., Fuentes, M., Geer, A., Haimberger, L., Healy, S., Hogan,
642 R. J., Hólm, E., Janisková, M., Keeley, S., Laloyaux, P., Lopez, P., Lupu, C., Radnoti, G., Rosnay,
643 P., Rozum, I., Vamborg, F., Villaume, S. and Thépaut, J. N.: The ERA5 global reanalysis, Q. J. R.
644 Meteorol. Soc., 146(730), 1999–2049, doi:10.1002/qj.3803, 2020.

645 Hughes, M., Mahoney, K. M., Neiman, P. J., Moore, B. J., Alexander, M. and Ralph, F. M.: The
646 landfall and inland penetration of a flood-producing atmospheric river in Arizona. Part II: Sensitivity

https://doi.org/10.5194/essd-2020-397
Preprint. Discussion started: 19 February 2021

of modeled precipitation to terrain height and atmospheric river orientation, J. Hydrometeorol., 15(5), 1954–1974, doi:10.1175/JHM-D-13-0176.1, 2014.

Hunt, K. M. R., Curio, J., Turner, A. G. and Schiemann, R.: Subtropical Westerly Jet influence on occurrence of Western Disturbances and Tibetan Plateau Vortices, Geophys. Res. Lett., 45(16), 8629–8636, doi:10.1029/2018GL077734, 2018a.

Hunt, K. M. R., Turner, A. G. and Shaffrey, L. C.: The evolution, seasonality and impacts of western disturbances: On Western Disturbances, Q. J. R. Meteorol. Soc., 144(710), 278–290, doi:10.1002/qj.3200, 2018b.

Huss, M. and Hock, R.: Global-scale hydrological response to future glacier mass loss, Nat. Clim. Change, 8(2), 135–140, doi:10.1038/s41558-017-0049-x, 2018.

Immerzeel, W. W., Wanders, N., Lutz, A. F., Shea, J. M. and Bierkens, M. F. P.: Reconciling high-altitude precipitation in the upper Indus basin with glacier mass balances and runoff, Hydrol. Earth Syst. Sci., 19(11), 4673–4687, doi:10.5194/hess-19-4673-2015, 2015.

Immerzeel, W. W., Lutz, A. F., Andrade, M., Bahl, A., Biemans, H., Bolch, T., Hyde, S., Brumby, S., Davies, B. J., Elmore, A. C., Emmer, A., Feng, M., Fernández, A., Haritashya, U., Kargel, J. S., Koppes, M., Kraaijenbrink, P. D. A., Kulkarni, A. V., Mayewski, P. A., Nepal, S., Pacheco, P., Painter, T. H., Pellicciotti, F., Rajaram, H., Rupper, S., Sinisalo, A., Shrestha, A. B., Viviroli, D., Wada, Y., Xiao, C., Yao, T. and Baillie, J. E. M.: Importance and vulnerability of the world's water towers, Nature, 577(7790), 364–369, doi:10.1038/s41586-019-1822-y, 2020.

Kamae, Y., Mei, W., Xie, S.-P., Naoi, M. and Ueda, H.: Atmospheric rivers over the northwestern Pacific: Climatology and interannual variability, J. Clim., 30(15), 5605–5619, doi:10.1175/JCLI-D-16-0875.1, 2017.

Krishnan, R., Shrestha, A. B., Ren, G., Rajbhandari, R., Saeed, S., Sanjay, J., Syed, M. A., Vellore, R., Xu, Y., You, Q. and Ren, Y.: Unravelling climate change in the Hindu Kush Himalaya: Rapid warming in the mountains and increasing extremes, in The Hindu Kush Himalaya Assessment, edited by P. Wester, A. Mishra, A. Mukherji, and A. B. Shrestha, pp. 57–97, Springer International Publishing, Cham., 2019.

Laghari, J. R.: Climate change: Melting glaciers bring energy uncertainty, Nature, 502(7473), 617–618, doi:10.1038/502617a, 2013.

Lakshmi, D. D. and Satyanarayana, A. N. V.: Influence of atmospheric rivers in the occurrence of devastating flood associated with extreme precipitation events over Chennai using different reanalysis data sets, Atmospheric Res., 215, 12–36, doi:10.1016/j.atmosres.2018.08.016, 2019.

Lakshmi, D. D., Satyanarayana, A. N. V. and Chakraborty, A.: Assessment of heavy precipitation events associated with floods due to strong moisture transport during summer monsoon over India, J. Atmospheric Sol.-Terr. Phys., 189, 123–140, doi:10.1016/j.jastp.2019.04.013, 2019.

Lamjiri, M. A., Dettinger, M. D., Ralph, F. M. and Guan, B.: Hourly storm characteristics along the U.S. West Coast: Role of atmospheric rivers in extreme precipitation: Storm characteristics in U.S. West Coast, Geophys. Res. Lett., 44(13), 7020–7028, doi:10.1002/2017GL074193, 2017.

https://doi.org/10.5194/essd-2020-397
Preprint. Discussion started: 19 February 2021

685 Laskhmi, D. D. and Satyanarayana, A. N. V.: Climatology of landfalling atmospheric Rivers and
686 associated heavy precipitation over the Indian coastal regions, Int. J. Climatol., joc.6540,
687 doi:10.1002/joc.6540, 2020.

688 Lavers, D. A. and Villarini, G.: Atmospheric rivers and flooding over the central United States, J.
689 Clim., 26(20), 7829–7836, doi:10.1175/JCLI-D-13-00212.1, 2013a.

690 Lavers, D. A. and Villarini, G.: The nexus between atmospheric rivers and extreme precipitation
691 across Europe: ARs and extreme European precipitation, Geophys. Res. Lett., 40(12), 3259–3264,
692 doi:10.1002/grl.50636, 2013b.

693 Lavers, D. A. and Villarini, G.: The contribution of atmospheric rivers to precipitation in Europe and
694 the United States, J. Hydrol., 522, 382–390, doi:10.1016/j.jhydrol.2014.12.010, 2015a.

695 Lavers, D. A. and Villarini, G.: The relationship between daily European precipitation and measures
696 of atmospheric water vapour transport: Daily European precipitation and water vapour transport., Int.
697 J. Climatol., 35(8), 2187–2192, doi:10.1002/joc.4119, 2015b.

698 Lavers, D. A., Vallarini, G., Allan, R. P., Wood, E. . F. and Wade, A. J.: The detection of
699 atmospheric reanalyses and their links to British winter floods and the large-scale climatic
700 circulation., J. Geophys. Res. Atmospheres, 117(D20), doi:https://doi.org/10.1029/2012JD018027.,
701 2012.

702 Lavers, D. A., Allan, R. P., Villarini, G., Lloyd-Hughes, B., Brayshaw, D. J. and Wade, A. J.: Future
703 changes in atmospheric rivers and their implications for winter flooding in Britain, Environ. Res.
704 Lett., 8(3), 034010, doi:10.1088/1748-9326/8/3/034010, 2013.

705 Leung, L. R. and Qian, Y.: Atmospheric rivers induced heavy precipitation and flooding in the
706 western U.S. simulated by the WRF regional climate model: Atmospheric river, precipitation, flood.,
707 Geophys. Res. Lett., 36(3), n/a-n/a, doi:10.1029/2008GL036445, 2009.

708 Liang, J. and Yong, Y.: Climatology of atmospheric rivers in the Asian monsoon region, Int. J.
709 Climatol., joc.6729, doi:10.1002/joc.6729, 2020.

710 Litt, M., Shea, J., Wagnon, P., Steiner, J., Koch, I., Stigter, E. and Immerzeel, W.: Glacier ablation
711 and temperature indexed melt models in the Nepalese Himalaya, Sci. Rep., 9(1), 5264,
712 doi:10.1038/s41598-019-41657-5, 2019.

713 Lora, J. M., Shields, C. A. and Rutz, J. J.: Consensus and Disagreement in Atmospheric River
714 Detection: ARTMIP Global Catalogues, Geophys. Res. Lett., 47(20), doi:10.1029/2020GL089302,
715 2020.

716 Mandal, A., Ramanathan, A., Azam, M. F., Angchuk, T., Soheb, M., Kumar, N., Pottakkal, J. G.,
717 Vatsal, S., Mishra, S. and Singh, V. B.: Understanding the interrelationships among mass balance,
718 meteorology, discharge and surface velocity on Chhota Shigri Glacier over 2002–2019 using in situ
719 measurements, J. Glaciol., 66(259), 727–741, doi:10.1017/jog.2020.42, 2020.

720 Maussion, F., Scherer, D., Mölg, T., Collier, E., Curio, J. and Finkelnburg, R.: Precipitation
721 Seasonality and Variability over the Tibetan Plateau as Resolved by the High Asia Reanalysis*, J.
722 Clim., 27(5), 1910–1927, doi:10.1175/JCLI-D-13-00282.1, 2014.

https://doi.org/10.5194/essd-2020-397
Preprint. Discussion started: 19 February 2021

723 Mishra, V., Smoliak, B. V., Lettenmaier, D. P. and Wallace, J. M.: A prominent pattern of year-to-
724 year variability in Indian Summer Monsoon Rainfall, Proc. Natl. Acad. Sci., 109(19), 7213–7217,
725 doi:10.1073/pnas.1119150109, 2012.

726 Molden, D., Sharma, E., Shrestha, A. B., Chettri, N., Pradhan, N. S. and Kotru, .: Advancing
727 Regional and Transboundary Cooperation in the Conflict-Prone Hindu Kush–Himalaya, Mt. Res.
728 Dev., 37(4), 502–508, doi:10.1659/MRD-JOURNAL-D-17-00108.1, 2017.

729 Mölg, T., Maussion, F. and Scherer, D.: Mid-latitude westerlies as a driver of glacier variability in
730 monsoonal High Asia, Nat. Clim. Change, 4(1), 68–73, doi:10.1038/nclimate2055, 2014.

731 Momblanch, A., Papadimitriou, L., Jain, S. K., Kulkarni, A., Ojha, C. S. P., Adeloye, A. J. and
732 Holman, I. P.: Untangling the water-food-energy-environment nexus for global change adaptation in
733 a complex Himalayan water resource system, Sci. Total Environ., 655, 35–47,
734 doi:10.1016/j.scitotenv.2018.11.045, 2019.

735 Nayak, M. A., Azam, M. F, and Lyngwa, R. V. 2021: Atmospheric River Database for the Himalayas
736 , Zenodo, https://doi.org/10.5281/zenodo.4451901
737
738 Nayak, M. A. and Villarini, G.: A long-term perspective of the hydroclimatological impacts of
739 atmospheric rivers over the central United States., Water Resour. Res., 53(2), 1144–1166,
740 doi:10.1002/2016WR019033, 2017.

741 Nayak, M. A., Villarini, G. and Lavers, D. A.: On the skill of numerical weather prediction models to
742 forecast atmospheric rivers over the central United States: Skills of NWP models to forecast ARs.,
743 Geophys. Res. Lett., 41(12), 4354–4362, doi:10.1002/2014GL060299, 2014.

744 Nayak, M. A., Villarini, G. and Bradley, A. A.: Atmospheric rivers and rainfall during NASA's Iowa
745 Flood Studies (IFloodS) Campaign, J. Hydrometeorol., 17(1), 257–271, doi:10.1175/JHM-D-14-
746 0185.1, 2016.

747 Neiman, P. J., Ralph, F. M., Wick, G. A., Kuo, Y., Wee, T., Ma, Z., Taylor, G. H. and Dettinger, M.
748 D.: Diagnosis of an Intense Atmospheric River Impacting the Pacific Northwest: Storm Summary
749 and Offshore Vertical Structure Observed with COSMIC Satellite Retrievals, Mon. Weather Rev.,
750 136(11), 4398–4420, doi:10.1175/2008MWR2550.1, 2008a.

751 Neiman, P. J., Ralph, F. M., Wick, G. A., Lundquist, J. D. and Dettinger, M. D.: Meteorological
752 characteristics and overland precipitation impacts of atmospheric rivers affecting the West Coast of
753 North America based on eight years of SSM/I satellite observations, J. Hydrometeorol., 9(1), 22–47,
754 doi:10.1175/2007JHM855.1, 2008b.

755 Neiman, P. J., Ralph, F. M., Moore, B. J., Hughes, M., Mahoney, K. M., Cordeira, J. M. and
756 Dettinger, M. D.: The Landfall and inland penetration of a flood-producing atmospheric river in
757 Arizona. Part I: Observed synoptic-scale, orographic, and hydrometeorological characteristics, J.
758 Hydrometeorol., 14(2), 460–484, doi:10.1175/JHM-D-12-0101.1, 2013.

759 Newell, R. E., Newell, N. E., Zhu, Y. and Scott, C.: Tropospheric rivers? - A pilot study, Geophys.
760 Res. Lett., 19(24), 2401–2404, doi:10.1029/92GL02916, 1992.

761 Nuimura, T., Sakai, A., Taniguchi, K., Nagai, H., Lamsal, D., Tsutaki, S., Kozawa, A., Hoshina, Y.,
762 Takenaka, S., Omiya, S., Tsunematsu, K., Tshering, P. and Fujita, K.: The GAMDAM glacier

https://doi.org/10.5194/essd-2020-397
Preprint. Discussion started: 19 February 2021

763 inventory: a quality-controlled inventory of Asian glaciers, The Cryosphere, 9(3), 849–864,
764 doi:10.5194/tc-9-849-2015, 2015.

765 Pai, D., Sridhar, L., Rajeevan, M., Sreejith, O. P., Satbhai, N. S. and Mukhopadhyay, B.:
766 Development of a new high spatial resolution (0.25° × 0.25°) long period (1901-2010) daily gridded
767 rainfall data set over India and its comparison with existing data sets over the region, Mausam, 65,
768 1–18, 2014.

769 Pan, M. and Lu, M.: A novel atmospheric river identification algorithm, Water Resour. Res., 55(7),
770 6069–6087, doi:10.1029/2018WR024407, 2019.

771 Paul, S., Ghosh, S., Oglesby, R., Pathak, A., Chandrasekharan, A. and Ramsankaran, R.: Weakening
772 of Indian Summer Monsoon Rainfall due to changes in land use land cover, Sci. Rep., 6(1), 32177,
773 doi:10.1038/srep32177, 2016.

774 Pörtner, H. O., Roberts, D. C., Masson-Delmotte, V., Zhai, P., Tignor, M., Poloczanska, E.,
775 Mintenbeck, K., Nicolai, M., Okem, A., Petzold, J. and Rama, B.: IPCC special report on the ocean
776 and cryosphere in a changing climate. IPCC Intergovernmental Panel on Climate Change, 2019.

777 Pritchard, H. D.: Asia's shrinking glaciers protect large populations from drought stress, Nature,
778 569(7758), 649–654, doi:10.1038/s41586-019-1240-1, 2019.

779 Ralph, F. M., Neiman, P. J. and Wick, G. A.: Satellite and CALJET aircraft observations of
780 atmospheric rivers over the eastern North Pacific Ocean during the winter of 1997/98., Mon.
781 Weather Rev., 132(7), 1721–1745, doi:https://doi.org/10.1175/1520-
782 0493(2004)132<1721:SACAOO>2.0.CO;2, 2004.

783 Ralph, F. M., Neiman, P. J., Kiladis, G. N., Weickmann, K. and Reynolds, D. W.: A multiscale
784 observational case study of a Pacific atmospheric river exhibiting tropical–extratropical connections
785 and a mesoscale frontal wave, Mon. Weather Rev., 139(4), 1169–1189,
786 doi:10.1175/2010MWR3596.1, 2011.

787 Ralph, F. M., Coleman, T., Neiman, P. J., Zamora, R. J. and Dettinger, M. D.: Observed impacts of
788 duration and seasonality of atmospheric-river landfalls on soil moisture and runoff in coastal
789 northern California, J. Hydrometeorol., 14(2), 443–459, doi:10.1175/JHM-D-12-076.1, 2013.

790 Ralph, F. M., Dettinger, M. D., Cairns, M. M., Galarneau, T. J. and Eylander, J.: Defining
791 "Atmospheric River": How the Glossary of Meteorology helped resolve a debate, Bull. Am.
792 Meteorol. Soc., 99(4), 837–839, doi:10.1175/BAMS-D-17-0157.1, 2018.

793 Ralph, F. M., Rutz, J. J., Cordeira, J. M., Dettinger, M., Anderson, M., Reynolds, D., Schick, L. J.
794 and Smallcomb, C.: A Scale to Characterize the Strength and Impacts of Atmospheric Rivers, Bull.
795 Am. Meteorol. Soc., 100(2), 269–289, doi:10.1175/BAMS-D-18-0023.1, 2019.

796 Ramos, A. M., Nieto, R., Tomé, R., Gimeno, L., Trigo, R. M., Liberato, M. L. R. and Lavers, D. A.:
797 Atmospheric rivers moisture sources from a Lagrangian perspective, Earth Syst. Dyn., 7(2), 371–
798 384, doi:10.5194/esd-7-371-2016, 2016.

799 Rao, K. N., Narasimha, R. and Narayanan, M. A. B.: The 'bursting' phenomenon in a turbulent
800 boundary layer, J. Fluid Mech., 48(2), 339–352, doi:10.1017/S0022112071001605, 1971.

https://doi.org/10.5194/essd-2020-397
Preprint. Discussion started: 19 February 2021

Rao, Y. P., Srinivasan, V. and Raman, S.: "Forecasting manual." Part-II, Discussion of typical synoptic weather situation, winter-western disturbances and their associated features. FMU Report No. III-1.1, India Meteorological Department. Delhi, India, 1969.

Romshoo, S. A., Altaf, S., Rashid, I. and Dar, R. A.: Climatic, geomorphic and anthropogenic drivers of the 2014 extreme flooding in the Jhelum basin of Kashmir, India, Geomat. Nat. Hazards Risk, 9(1), 224–248, doi:10.1080/19475705.2017.1417332, 2018.

Rutz, J. J., Steenburgh, W. J. and Ralph, F. M.: Climatological characteristics of atmospheric rivers and their inland penetration over the Western United States, Mon. Weather Rev., 142(2), 905–921, doi:10.1175/MWR-D-13-00168.1, 2014.

Schiemann, R., Lüthi, D., Vidale, P. L. and Schär, C.: The precipitation climate of Central Asia—intercomparison of observational and numerical data sources in a remote semiarid region, Int. J. Climatol., 28(3), 295–314, doi:10.1002/joc.1532, 2008.

Shen, H. and Poulsen, C. J.: Precipitation δ18O on the Himalaya-Tibet orogeny and its relationship to surface elevation, preprint, Climate Modelling/Modelling only/Cenozoic., 2018.

Shields, C. A., Rutz, J. J., Leung, L. A., Ralph, F. M., Wehner, M., Kawzenuk, B., Lora, J. M., McClenny, E., Osborne, T., Payne, A. E., Ullrich, P., Gershunov, A., Goldenson, N., Guan, B., Qian, Y., Ramos, A. M., Sarangi, C., Sellars, S., Gorodetskaya, I., Kashinath, K., Kurlin, V., Mahoney, K., Muszynski, G., Pierce, R., Subramanian, A. C., D., R., D., D., Walton, D., Wick, G., Wilson, A., Lavers, D. A., Prabhat, Collow, A., Krishnan, H., Magnusdottir, G. and Nguyen, P.: Atmospheric river tracking method intercomparison project (ARTMIP): Project goals and experimental design, Geosci. Model Dev., 11(6), 2455–2474, doi:10.5194/gmd-11-2455-2018, 2018.

Sodemann, H. and Stohl, A.: Moisture origin and meridional transport in atmospheric rivers and their association with multiple cyclones, Mon. Weather Rev., 141(8), 2850–2868, doi:10.1175/MWR-D-12-00256.1, 2013.

Steinschneider, S. and Brown, C.: Dynamic reservoir management with real-option risk hedging as a robust adaptation to nonstationary climate: Real-option risk hedging and climate change, Water Resour. Res., 48(5), doi:10.1029/2011WR011540, 2012.

Steinschneider, S., McCrary, R., Wi, S., Mulligan, K., Mearns, L. O. and Brown, C.: Expanded decision-scaling framework to select robust long-term water-system plans under hydroclimatic uncertainties, J. Water Resour. Plan. Manag., 141(11), 04015023, doi:10.1061/(ASCE)WR.1943-5452.0000536, 2015.

Stohl, A., Forster, C. and Sodemann, H.: Remote sources of water vapor forming precipitation on the Norwegian west coast at 60°N–a tale of hurricanes and an atmospheric river, J. Geophys. Res. Atmospheres, 115(D5), doi:https://doi.org/10.1029/2007JD009006, 2008.

Thapa, K., Endreny, T. A. and Ferguson, C. R.: Atmospheric rivers carry nonmonsoon extreme precipitation into Nepal, J. Geophys. Res. Atmospheres, 123(11), 5901–5912, doi:10.1029/2017JD027626, 2018.

Veh, G., Korup, O., von Specht, S., Roessner, S. and Walz, A.: Unchanged frequency of moraine-dammed glacial lake outburst floods in the Himalaya, Nat. Clim. Change, 9(5), 379–383, doi:10.1038/s41558-019-0437-5, 2019.

https://doi.org/10.5194/essd-2020-397
Preprint. Discussion started: 19 February 2021

841 Waliser, D. and Guan, B.: Extreme winds and precipitation during landfall of atmospheric rivers,
842 Nat. Geosci., 10(3), 179–183, doi:10.1038/ngeo2894, 2017.

843 Webster, P. J., Magaña, V. O., Palmer, T. N., Shukla, J., Tomas, R. A., Yanai, M. and Yasunari, T.:
844 Monsoons: Processes, predictability, and the prospects for prediction, J. Geophys. Res. Oceans,
845 103(C7), 14451–14510, doi:10.1029/97JC02719, 1998.

846 Wick, G. A., Neiman, P. J. and Ralph, F. M.: Description and validation of an automated objective
847 technique for identification and characterization of the integrated water vapor signature of
848 atmospheric rivers, IEEE Trans. Geosci. Remote Sens., 51(4), 2166–2176,
849 doi:10.1109/TGRS.2012.2211024, 2013.

850 Wille, J. D., Favier, V., Dufour, A., Gorodetskaya, I. V., Turner, J., Agosta, C. and Codron, F.: West
851 Antarctic surface melt triggered by atmospheric rivers, Nat. Geosci., 12(11), 911–916,
852 doi:10.1038/s41561-019-0460-1, 2019.

853 Yang, Y., Zhao, T., Ni, G. and Sun, T.: Atmospheric rivers over the Bay of Bengal lead to northern
854 Indian extreme rainfall: Atmospheric rivers over the Bay of Bengal, Int. J. Climatol., 38(2), 1010–
855 1021, doi:10.1002/joc.5229, 2018.

856 Young, A. L., Skelly, K. T. and Cordeira, J. M.: High-impact hydrologic events and atmospheric
857 rivers in California: An investigation using the NCEI Storm Events Database., Geophys. Res. Lett.,
858 44(7), 3393–3401, doi:10.1002/2017GL073077, 2017.

859 Zhou, Y., Kim, H. and Guan, B.: Life cycle of Atmospheric rivers: Identification and climatological
860 characteristics, J. Geophys. Res. Atmospheres, 123(22), doi:10.1029/2018JD029180, 2018.

861 Zhu, Y. and Newell, R. E.: A proposed algorithm for moisture fluxes from atmospheric rivers., Mon.
862 Weather Rev., 126(3), 725–735., doi:https://doi.org/10.1175/1520-
863 0493(1998)126<0725:APAFMF>2.0.CO;2, 1998.

864